ENERGY STORAGE IN THE PRIMARY STEP OF THE PHOTOCYCLE OF BACTERIORHODOPSIN

ROBERT R. BIRGE AND THOMAS M. COOPER
Department of Chemistry, University of California, Riverside, California 92521

ABSTRACT A pulsed-dye laser low temperature photocalorimeter is used to study the enthalpy differences between light-adapted bacteriorhodopsin (bR_{568}) and its primary photoproduct (K) at 77 K. A key feature of our experimental method is the use of the laser-induced photostationary state as an internal reference. Analyses of the forward (bR → K), reverse (K → bR), and mixed (bR ⇌ K) photoreactions were carried out to measure $\Delta H_{12} = E_K - E_{bR}$. All three experiments yielded identical values of ΔH_{12} within experimental error ($\Delta H_{12}^{ave} = 15.8 \pm 2.5$ kcal mol^{-1}). Accordingly, the primary event in the photocycle of light-adapted bacteriorhodopsin stores ~30% of the absorbed photon energy at the 568-nm absorption maximum. We observe that the quantum yields ϕ_1^f(bR → K) and ϕ_2^r(K → bR) add up to unity within experimental error: $\phi_1^f + \phi_2^r = 1.02 \pm 0.19$ for ϕ_1^f in the range 0.28–0.33. A theoretical analysis of energy storage in K suggests that at least one-half of the enthalpy difference between K and bR is associated with charge separation accompanying chromophore isomerization.

INTRODUCTION

Bacteriorhodopsin is the light-harvesting protein of the purple membrane of the halophilic microorganism *Halobacterium halobium* (Lozier et al., 1975; Lozier and Niederberger, 1977). This protein exists in two stable forms, one containing all-*trans* retinal and the other containing 13-*cis* retinal. In the dark, both forms are present in approximately equal proportions. Under continuous exposure to visible light, the dark adapted form containing 13-*cis* retinal (bR_{548}) is photoisomerized to the light-adapted form containing all-*trans* retinal (bR_{568}). The latter undergoes a photochemical cycle that is responsible for transporting protons across the membrane (Fig. 1) (for recent reviews see Stoeckenius et al., 1979; Ottolenghi, 1980; Birge, 1981).

An interesting feature of this photochemical cycle is its similarity in its early stages to the photobleaching sequence of rhodopsin (Fig. 1). In particular, both reaction paths involve the extremely rapid photochemical formation of bathochromically shifted primary photoproducts

$$bR_{568} \xrightarrow{h\nu} K \longrightarrow \text{thermal intermediates}$$

$$\text{rhodopsin} \xrightarrow{h\nu} \text{bathorhodopsin} \longrightarrow \text{thermal intermediates.}$$

The primary photoproducts then undergo a series of thermal (dark) reactions. It is generally believed that the primary events associated with the above reaction sequences involve the isomerization of the retinyl chromophore followed by a fast proton translocation within the ground state manifold (Honig, 1982). However, the molecular details and, in fact, the chronology of events within the primary step remain a subject of debate.

The relative energy of the primary photoproduct (K or bathorhodopsin) is an important experimental parameter. It represents the amount of energy stored in the primary event and the total energy available for driving the subsequent thermal reactions. Cooper (1979) has measured the enthalpy of bathorhodopsin to be ~35 kcal mol^{-1} higher than rhodopsin. This energy difference indicates that the primary step of visual excitation stores more than 60% of the absorbed photon energy at the 500-nm absorption maximum. The present investigation measures the energy storage associated with the primary step in the photocycle of light-adapted bacteriorhodopsin. Our analysis indicates that the enthalpy of the K intermediate is ~16 kcal mol^{-1} higher than bR_{568}. Accordingly, the primary event in the photocycle of light-adapted bacteriorhodopsin stores ~30% of the absorbed photon energy at the 568-nm absorption maximum. This percentage is roughly half of that observed for the primary event in the rhodopsin bleaching sequence. We analyze this difference below and suggest that it is consistent with the concept that a significant proportion of the energy stored in the primary step is associated with charge separation accompanying the photoisomerization of the retinyl protonated Schiff base.

MATERIALS AND METHODS

Bacteriorhodopsin was isolated from the R1 (or M1) strain of *Halobacterium halobium* following the procedures of Becher and Cassim (1975). The protein was dissolved in 2:1 glycerol/water (vol/vol) to produce an optical density of 8 ± 0.2 at 568 nm in a 1-cm pathlength cell at room temperature. This concentration was used in the calorimetry experiments so that roughly an order of magnitude more bacteriorhodopsin was

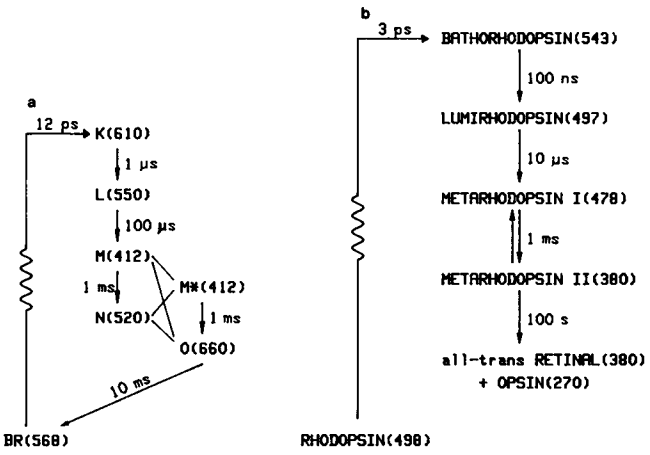

FIGURE 1 (*a*) The photochemical cycle of light-adapted bacteriorhodopsin and (*b*) the bleaching sequence of rhodopsin are shown. Relative free energies are approximately related to vertical position in the figure. Absorption maxima in nanometers are given in parentheses. The exact chronology of the dark reactions in bacteriorhodopsin is not yet precisely known. The formation times of the primary photoproducts and order of magnitude estimates of the dark reaction times are for ambient temperature. In the present paper we will use the symbol bR to represent bR_{568} and the symbol K to represent K_{610}.

present than photons entering the photocalorimeter cell during a given laser pulse.

The pulsed-dye laser photocalorimeter is schematically shown in Fig. 2. The calorimeter portion (C in Fig. 2) is similar to the low temperature system designed by Cooper (1979, 1982) to study the primary event of the rhodopsin photobleaching sequence. A scale drawing of the calorimeter cell is shown in Fig. 3. The sample of bacteriorhodopsin is placed in the sample cell (S in Fig. 2) and irradiated using the filtered xenon lamp for 20 min to light-adapt the protein. A solution of 2:1 glycerol/water (vol/vol) is placed in the reference cell (R). Liquid nitrogen is then added to the Dewar flask containing the calorimeter, and the system is allowed to equilibrate at 77 K for ~2 h to minimize thermal gradients. The xenon lamp filters are changed depending upon experiment. To study the forward reaction, (bR → K), a Corning 2-59 ($\lambda > 620$ nm) filter (Corning Glass Works, Science Products Div., Corning, NY) is used to convert any K intermediate present photochemically back to bR. This irradiation technique produces >97% bR. To study the reverse reaction, (K → bR), a Ditric 500-nm interference filter (Ditric Optics, Inc., Hudson, MA) is used to produce a photostationary state mixture containing 28% K and 72% bR (Hurley and Ebrey, 1978). The lamp assembly is turned off (or the shutter is closed, Fig. 2) before firing the laser.

A pulsed laser is used to irradiate the sample to determine enthalpy changes accompanying the forward or reverse reactions. The voltage signal from the calorimeter is obtained by subtracting the voltage of the reference cell peltier receivers from the voltage of the sample cell peltier receivers (Fig. 2) using a PAR model 113 preamplifier (EG&G Princeton Applied Research Corp., Princeton, NJ). The reference cell is used to remove spurious voltage signals due to the small thermal gradients that exist in the brass heat sink (Fig. 3). The integral of the voltage signal is proportional to the heat given off by the sample following absorption of the pulsed laser light. Typical signals for the forward and reverse reactions are shown in Fig. 4. Note that the temporal response of the signal is due entirely to the calorimeter time constant (~25 s) because the duration of the laser pulse is ~0.4 µs and the primary event occurs on a picosecond time scale (Kaufmann et al., 1978). The sloping baseline is due to small temperature gradients in the brass heat sink. Theoretically, these gradients should be removed by subtracting the reference cell voltage (see above), but in practice the slight mismatch between the

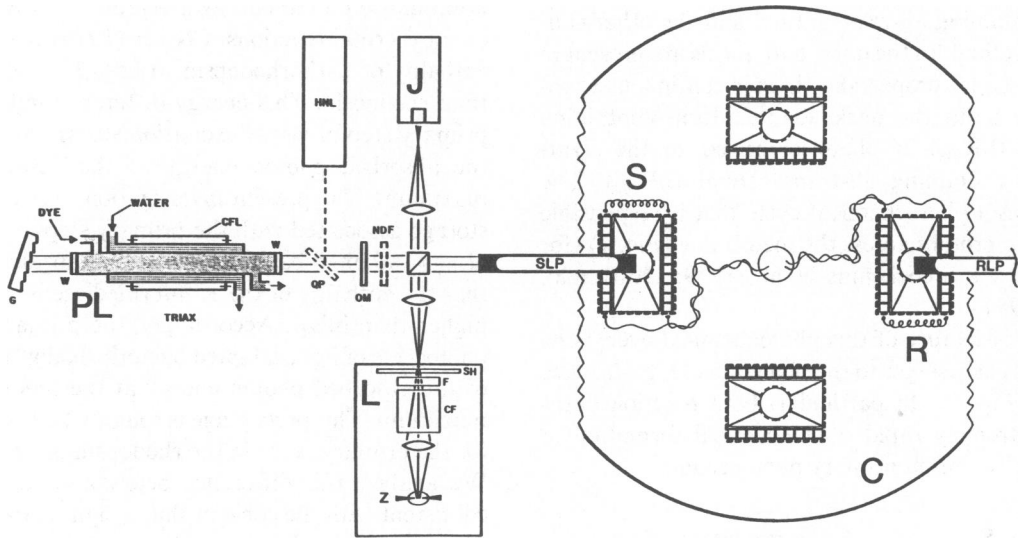

FIGURE 2 The pulsed tunable dye laser low temperature photocalorimeter. The pulsed laser (PL) is a Phase-R corporation (New Durham, NH) DL2100C triaxial (TRIAX) flashlamp-pumped tunable dye laser modified as described by Bennett and Birge (1980). The pulse energy is monitored using a Molectron model J3 pyroelectric joulemeter (J) (Molectron Corp., Sunnyvale CA). The desired photostationary state mixture is obtained using the xenon lamp and filter combination (L). Light is directed into the sample cell (S) of the calorimeter (C) using a fiber optics light guide (SLP). An identical light guide (RLP) is inserted into the reference call (R), but is capped at the external input to prevent light from entering. The calorimeter (C) is placed inside a large 10-l Dewar flask (not shown) and the Dewar flask is filled with liquid nitrogen. A copper Faraday cage surrounds the entire Dewar flask and the light guides and the shielded cables from the sample and reference cells are brought out of the top of the Dewar flask assembly through a large brass heat sink that is also immersed in liquid nitrogen. The remaining symbols are used to represent the following components: G, sine-bar drive diffraction grating; W, antireflection coated windows; CFL, coaxial flashlamp; QP, quartz plate; HNL, helium neon alignment laser; OM, 50% reflecting output mirror; NDF, neutral density filter(s); SH, shutter (closed before firing the laser); F, bandpass or interference filter; CF, broadband chemical filter to remove ultraviolet light <400 nm and visible light >800 nm; Z, 100-W xenon lamp.

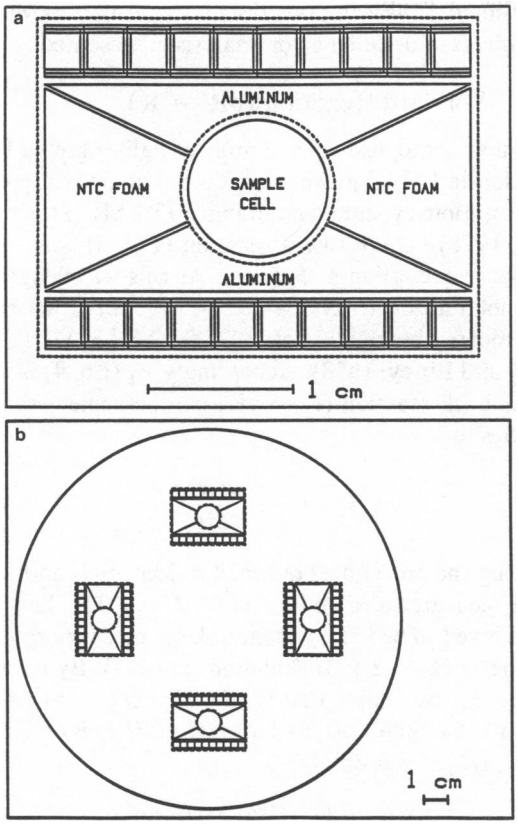

FIGURE 3 (*a*) Scale drawings of an individual calorimeter cell and (*b*) the bottom portion of the brass heat sink containing the four symmetrically arranged cells. The sample cell is thin walled stainless steel which is polished on the inside to maximize reflectivity. The nonthermally conducting foam (NTC foam) is used to prevent heat loss directly into the brass heat sink. Heat is directed using the aluminum blocks onto the inner surfaces of two solid-state thermoelectric detectors (950-71; Borg-Warner Electronics, Ithaca, NY), which are wired in series. These detectors are represented by the rectangular shapes with vertical connecting bars to schematically represent the individual thermoelectric elements.

sample and reference cells leads to a sloping baseline. Accordingly, a computer program was used to fit the baseline to a straight line using least squares regression and the integral was numerically evaluated after subtracting the calculated baseline.

The integral of the calorimeter signal, I_v, is numerically evaluated over the following limits

$$I_v = \int_{t_\ell}^{t_\ell + 3\tau} V(t)\,dt, \tag{1}$$

where $V(t)$ is the observed voltage response function after baseline subtraction (Fig. 4) and the integration is carried out from time t_ℓ, the time the laser is fired, to $t_\ell + 3\tau$, where τ is the calorimeter response time constant (3τ = 75 s). These limits were specified to optimize the signal-to-noise ratio of the numerical integral determination. As can be seen by reference to the baseline corrected response curves shown in curves *b* and *d* of Fig. 4, the voltage signal present 75 s after the laser pulse is dominated by thermal noise.

The above integral can be related to the reaction energetics of the protein by the equation

$$I_v = kN(\Delta E^{\lambda}_{\text{pulse}})\Gamma, \tag{2}$$

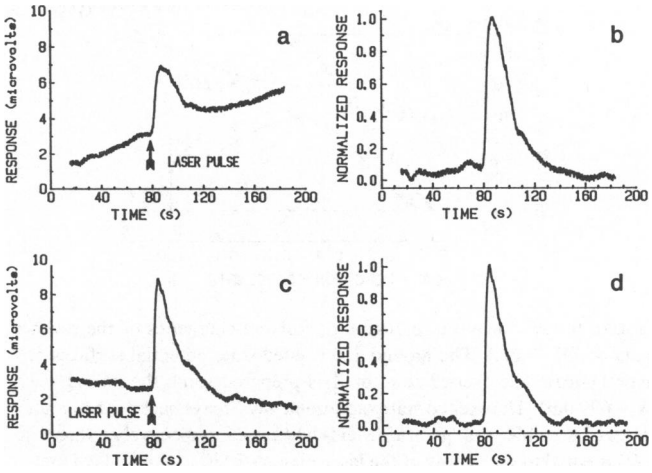

FIGURE 4 Typical calorimeter voltage signals ($S - R$) obtained from studying (*a*) the forward (bR → K) reaction and (*c*) the back (K → bR) reaction. Laser pulse energies were ~3 mJ in both examples. Curves *b* and *d* display the normalized signals after baseline subtraction for curves *a* and *c*, respectively.

where k is the calorimeter response function (assumed to remain constant during a given experiment), N is the number of photons in the laser pulse, $\Delta E^{\lambda}_{\text{pulse}}$ is the energy/mol of the laser photons [$\Delta E^{\lambda}_{\text{pulse}}$ (kcal mol^{-1}) = 28,590/λ(nm)], and Γ is the dimensionless molecular response function given by,

$$\Gamma = \left[\alpha_\lambda\left(1 - \phi_1^f \frac{\Delta H_{12}}{\Delta H_2^f}\right)\right] + \left[(1 - \alpha_\lambda)\left(1 + \phi_2^r \frac{\Delta H_{12}}{\Delta H_1^r}\right)\right] \tag{3}$$

where

$$\alpha_\lambda = \{[\text{bR}]\epsilon^{\lambda}_{\text{bR}}\}/\{[\text{bR}]\epsilon^{\lambda}_{\text{bR}} + [\text{K}]\epsilon^{\lambda}_{\text{K}}\}, \tag{4}$$

where ϕ_1^f is the bR → K quantum yield, ϕ_2^r is the K → bR quantum yield, and the remaining terms in Eq. 3 are defined in Figs. 5 and 6. The terms appearing in Eq. 4 are: [bR], the molar concentration of bR; $\epsilon^{\lambda}_{\text{bR}}$, the molar absorptivity of bR at the laser excitation wavelength, λ; and [K] and $\epsilon^{\lambda}_{\text{K}}$ are similarly defined for K.

A key feature of the present experimental approach is the use of the laser-induced photostationary state (LIPS) as an experimental control. The LIPS is generated by sending 20 or more, 5–10-mJ laser pulses into

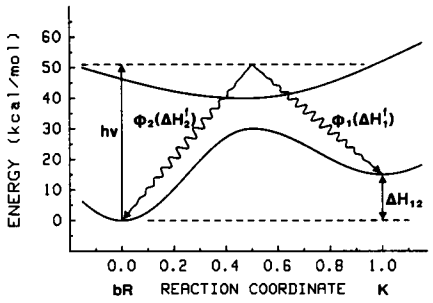

FIGURE 5 A schematic representation of the energetics of the forward reaction (bR → K). The ground and excited state potential surfaces are hypothetical. The excited state of bR is prepared using the pulsed laser (λ = 565 nm). The excited state radiationlessly decays back to the ground states of K or bR with quantum yields of ϕ_1^f or ϕ_2^r, respectively. Note that ΔH_2^f is equal to the energy of the laser photons [$\Delta E^{\lambda}_{\text{pulse}}$ = 50.6 kcal mol^{-1} (λ = 565 nm)] and $\Delta H_1^f = \Delta H_2^f - \Delta H_{12}$, where $\Delta H_{12} = E_{\text{K}} - E_{\text{bR}}$.

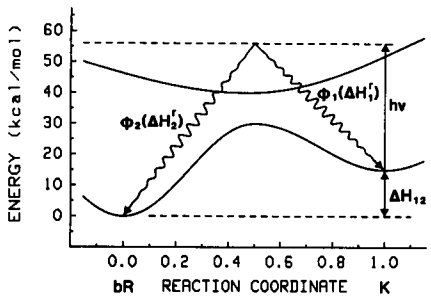

FIGURE 6 A schematic representation of the energetics of the reverse reaction (K → bR). The ground and excited state potential surfaces are hypothetical. The excited state of K is prepared using the pulsed laser (λ = 699 nm). The excited state radiationlessly decays back to the ground states of K or bR with quantum yields of ϕ_1^r or ϕ_2^r, respectively. Note that ΔH_1^r is equal to the energy of the laser photons [$\Delta E_{pulse}^{\lambda}$ = 40.9 kcal mol^{-1} (λ = 699 nm)] and $\Delta H_2^r = \Delta H_1^r + \Delta H_{12}$.

the sample until the energy normalized voltage response integral, I_v/N, remains constant. The salient characteristics of the LIPS is that all of the energy absorbed by the sample is returned as heat (no net reactions take place). Accordingly, the molecular response function, Γ, equals unity; and

$$(I_v)_{cntl} = kN\,\Delta E_{pulse}^{\lambda}. \tag{5}$$

Combining Eqs. 2 and 5 gives

$$\frac{[(I_v/N)_{expt}^{\lambda}]_{ave}}{[(I_v/N)_{cntl}^{\lambda}]_{ave}} = \Gamma_{obsvd}^{\lambda}. \tag{6}$$

The experimental value, Γ_{obsvd}^{λ}, is equated to the right-hand side of Eq. 3 to determine the unknown values of ΔH (see Results).

We summarize our experimental procedures below. (*a*) The xenon lamp assembly (L in Fig. 2) is used to convert the light-adapted bacteriorhodopsin to 97% bR (λ > 620 nm; to study the forward reaction) or 28% K (λ = 500 nm; to study the reverse and mixed reactions). After ~20 min the shutter is closed. (*b*) The flashlamp pumped dye laser (PL in Fig. 2) is fired to produce a single pulse at λ = 565 nm (to study the forward reaction), λ = 699 nm (to study the back reaction) or λ = 643 nm (to study the mixed reaction). The pulse energy (N) is measured using the Joulemeter (J in Fig. 2). The voltage response from the calorimeter (S voltage − R voltage) is recorded before, during, and after the laser pulse and the integral, I_v, is evaluated. (*c*) Steps *a* and *b* are repeated to provide measurements of $(I_v/N)_{expt}^{\lambda}$. (*d*) The dye laser is fired (5–10 mJ/pulse) 10–20 times at the same wavelength as used in step *b* to produce a photostationary state. Step *b* is then repeated (without using step *a* between pulses) to provide measurements of $(I_v/N)_{cntl}^{\lambda}$. (*e*) The average of the ratios measured in step *c* is divided by the average of the ratios measured in step *d* to yield an experimental measurement of Γ_{obsvd}^{λ} (see Eq. 6). (*f*) Eq. 3 is used to determine ΔH_{12}, where $\Delta H_{12} = E_K - E_{bR}$ (see Figs. 5 and 6 and following section for details).

RESULTS

Three experiments were carried out to determine the enthalpy difference between the K intermediate and bR. The first experiment studied the forward reaction (bR → K) ($\alpha \simeq 1$), the second studied the back reaction (K → bR) ($\alpha \simeq 0$), and the third studied the mixed (forward-back) reaction (bR ⇌ K). All of the calculations of ΔH_{12} ($=E_K - E_{bR}$) assume quantum yields of $\phi_1^f = 0.33$ and $\phi_2^r = 0.67$ (Figs. 5 and 6) (Hurley and Ebrey, 1978) except where noted. Following our discussion of the above three experiments, a detailed error analysis is presented.

Forward Reaction (bR → K)

Continuous irradiation of a sample of light-adapted bacteriorhodopsin (77 K) at wavelengths >620 nm will produce a photostationary state containing >97% bR (Hurley and Ebrey, 1978). The forward reaction (Fig. 5) was studied using laser excitation at 565 nm. At this wavelength, bR has a molar absorptivity of ~60,000 M^{-1} cm^{-1}, whereas K has a molar absorptivity of ~27,000 M^{-1} cm^{-1} (Fig. 4; Hurley and Ebrey, 1978). Accordingly, α_λ (Eq. 4) is >0.98 and the back reaction (K → bR) can be neglected. Eq. 3 simplifies to

$$\Gamma = 1 - \phi_1^f \frac{\Delta H_{12}}{\Delta H_2^f}. \tag{7}$$

Following the procedures outlined in Materials and Methods, we measured a value for Γ of 0.907 ± 0.021. This value was observed to be independent of laser pulse energy up to 6 mJ/pulse ($N \leq 2 \times 10^{16}$ photons pulse^{-1}). By reference to Fig. 5, we note that $\Delta H_2^f = \Delta E_{pulse}^{\lambda}$ = 28,590 (565 nm)$^{-1}$ = 50.6 kcal/mol and that ΔH_{12} ($E_K - E_{bR}$) = $\Delta H_2^f - \Delta H_1^f$. Accordingly,

$$\Delta H_{12} = (1 - \Gamma_{obsvd}^{\lambda})\,\Delta H_2^f/\phi_1^f, \tag{8}$$

which yields ΔH_{12} = 14.3 ± 3.2 assuming ϕ_1^f = 0.33. The results are summarized in Table I.

Reverse Reaction (K → bR)

The reverse reaction (Fig. 6) was studied by preparing a photostationary mixture containing 28% K by irradiating the sample at 500 nm (Hurley and Ebrey, 1978). Laser excitation at 699 nm was chosen because bR has negligible absorptivity, whereas the K species has a molar absorptivity of ~15,000 M^{-1} cm^{-1} at this wavelength. Accordingly, α_λ (Eq. 4) is <0.01 and Eq. 3 simplifies to

$$\Gamma = 1 + \phi_2^r(\Delta H_{12}/\Delta H_1^r). \tag{9}$$

Accordingly,

$$\Delta H_{12} = (\Gamma_{obsvd}^{\lambda} - 1)\Delta H_1^r/\phi_2^r, \tag{10}$$

where ΔH_1^r = 40.9 kcal mol^{-1} (λ = 699 nm), and ϕ_2^r = 0.67. The value of Γ_{obsvd}^{λ} was found to have a moderate pulse energy dependence below 5 mJ (Table II). This observation contrasts with the experimental results on the forward reaction for which no pulse energy dependence in Γ was observed below 6 mJ. The origin of the effect is traceable to the smaller number of absorbing species present for a 28% K solution excited at 699 nm. As the pulse energy increases, an increasing fraction of the K species is converted to bR and the sample exhibits a smaller absorptivity for photons arriving during the end of the laser pulse. This will tend to decrease Γ_{obsvd}^{λ} as pulse energy increases. The

TABLE I
MEASUREMENT OF THE ENTHALPY DIFFERENCE BETWEEN K and bR at −196°C

Parameter or condition	Reaction studied		
	Experiment 1 bR → K	Experiment 2 K → bR	Experiment 3 bR ⇌ K
Sample preparation wavelength*	>620	500	500
Sample mixture‡	>97% bR	28% K	28% K
Laser excitation wavelength§	565	699	643
Laser dye	Rhodamine 560	Oxazine 720	Rhodamine 640
α_λ (Eq. 4)‖	>0.98	<0.01	0.12 ± 0.01
Γ^{λ}_{obsvd}‖	0.907 ± 0.021	1.281 ± 0.037	1.196 ± 0.026
$\Delta H_{12} = E_K - E_{bR}$ ($kcal\ mol^{-1}$)¶	14.3 ± 3.2	17.2 ± 2.3	15.9 ± 2.1
ΔH_{12}(ave) ($kcal\ mol^{-1}$)**		15.8 ± 2.5	

*Wavelength output from the filtered xenon lamp (L in Fig. 2) measured in nanometers.
‡See Table I of Hurley and Ebrey (1978).
§Wavelength output from the flashlamp-pumped tunable dye laser (PL in Fig. 2 measured in nanometers). The absolute wavelength is accurate to better than ±1 nm and the laser output has a bandwidth of 0.02 nm.
‖See text for method of evaluation.
¶Calculated as described in the text assuming $\phi_1 = 0.33$ and $\phi_2 = 0.67$ (Hurley and Ebrey, 1978). Error range is based solely on observed error in Γ^{λ}_{obsvd}.
**Average of experiments 1, 2, and 3.

K → bR reaction occurs on a time scale significantly shorter than the laser pulse width (0.4 μs), and at high pulse intensities, the laser pulse creates its own photostationary state. To minimize this source of error, we use the Γ^{λ}_{obsvd} value corresponding to the lowest laser pulse energy to calculate $\Delta H_{12} = 17.2 \pm 2.3$ kcal mol^{-1}.

Mixed Forward and Reverse Reaction (bR ⇌ K)

The purpose of studying a mixed forward and reverse reaction is to provide an additional check on the validity of our model. Furthermore, it provides the opportunity to perform a global optimization of ΔH_{12} and ϕ_2 as a function of ϕ_1. This optimization is discussed in a separate section (see below).

TABLE II
EFFECT OF LASER PULSE ENERGY ON THE OBSERVED MOLECULAR RESPONSE FUNCTION (Γ) FOR 643- and 699-nm LASER EXCITATION

Pulse energy*	Γ_{obsvd} (λ_{ex} = 699 nm)‡	Γ_{obsvd} (λ_{ex} = 643 nm)‡
mJ		
1 ± 0.3	1.281 ± 0.037§	1.196 ± 0.026§
2 ± 0.3	1.274 ± 0.031	1.193 ± 0.033
3 ± 0.3	1.237 ± 0.028	1.181 ± 0.022
4 ± 0.3	1.209 ± 0.029	1.175 ± 0.017
5 ± 0.3	1.181 ± 0.019	1.164 ± 0.019
10 ± 1	—	1.103 ± 0.053

*The energy per pulse was measured using the joule meter (J in Fig. 2) simultaneously with measurement of voltage response from calorimeter circuit. The number of photons per pulse (N in Eqs. 2, 5, and 6) is related to the pulse energy in millijoules by the formula $N = 5.034 \times 10^{12} \cdot E(\text{mJ/pulse}) \cdot \lambda(\text{nm})$.
‡Average value of the observed molecular response function defined by Eq. 6 for values of laser pulse energy lying within the range given at left.
§Preferred value used to calculate ΔH_{12} (Table I).

The mixed reaction was studied by preparing a photostationary mixture of 28% K as in Experiment 2. Laser excitation at 643 nm was chosen so that the reverse reaction would be favored ($\alpha = 0.12 + 0.01$). The value of Γ^{λ}_{obsvd} exhibited a pulse energy dependence similar to that observed for the K → bR reaction (see Table II). As before, we choose the value corresponding to the lowest pulse energy range ($\Gamma^{\lambda}_{obsvd} = 1.196 \pm 0.026$) and an analysis of ΔH_{12} using Eq. 3 yields $\Delta H_{12} = 15.9 \pm 2.1$ kcal mol^{-1}. This value is very close to the median of the values obtained from measurements of the forward ($\Delta H_{12} = 14.3 \pm 3.2$) and the reverse ($\Delta H_{12} = 17.2 \pm 2.3$) reactions. All three measurements of ΔH_{12} agree within experimental error (Table I).

Analysis of Systematic Errors in Experimental Measurement of ΔH_{12}

There are a number of potential sources of systematic error inherent in our experimental procedures. The primary sources are discussed below and the magnitudes of the errors are estimated. We demonstrate that our experimental method serves to minimize systematic error by (*a*) using the laser-induced photostationary state as an internal control and (*b*) measuring ΔH_{12} as an average of the values obtained by monitoring the forward, mixed, and reverse reactions.

Systematic Error Due to Absorption of Laser Pulse by the Walls of the Sample Cell. The application of Eqs. 2–6 assumes that all of the laser photons that enter the sample solution are absorbed by the solute. We

attempted to maximize solute absorption (vs. cell wall absorption) by using a fiber optic light guide to direct the laser light into the center of the circular (top) area of the sample cell and adjusting the protein concentration such that the number of absorping species ($\sim 2 \times 10^{17}$) was roughly an order of magnitude larger than the number of photons per pulse. Furthermore, the inside surfaces of the stainless steel sample cell were polished to yield a >95% reflective surface at the laser wavelengths used in the present experiments. An approximate analysis using a ray tracing program (Birge, 1983) indicates that ~99% of the photons in a 565-nm, 3-mJ laser pulse that enter the solution will be abosrbed by bR_{568} in Experiment 1. This number drops to ~95% for a 699-nm, 3-mJ laser pulse absorbed by K (28%) in Experiment 2. Absorption of light by the cell walls will tend to shift Γ^{λ}_{obsvd} towards unity and will exhibit the same type of pulse energy dependence as observed due to saturation effects (see below and Table II). The source of the error is entirely associated with the $(I_v/N)^{\lambda}_{expt}$ value because $(I_v/N)^{\lambda}_{cntl}$ is invariant to the percent of light absorbed by the solute versus cell walls. However, the above ray tracing analysis as well as the observation that Experiment 2 yields a higher value of ΔH_{12} than Experiment 1 (the reverse would be expected if cell absorption were significant) suggest that error due to cell wall absorption is negligible.

Systematic Error Due to Optical Saturation. The importance of optical saturation has been examined in the discussion of Experiments 2 and 3 (see above and Table II). This phenomenon is well understood and can be compensated for by observing the pulse energy dependence in Γ^{λ}_{obsvd} and using pulse energies below the saturation level to measure ΔH_{12}. Analysis of Table II, however, indicates that a small amount of saturation may remain even at pulse energies below 2 mJ. Fortunately, these data also provide a means of calculating the worst case error and yield <0.6 kcal mol^{-1} for both Experiments 2 and 3 using 1-mJ pulse data (no saturation problems were observed for Experiment 1). Accordingly, optical saturation is not a significant source of systematic error relative to the random error inherent in measuring Γ^{λ}_{obsvd}.

Systematic Error Due to Side Reactions. Our calculations of ΔH_{12} assume that preparation of the excited electronic state (S_1^*) is followed by the formation of only two ground state species, bR or K. The possibility that a fraction of the excited state species (S_1^*) forms a pseudo intermediate called P-bR has been suggested (Gillbro et al., 1977; Kriebel et al., 1979; Gillbro and Sundström, 1983). Unfortunately, it is extremely difficult to estimate the concentration of P-bR in a photostationary mixture because the absorption spectrum is virtually identical to that of bR (Kriebel et al., 1979). Two pieces of evidence suggest that the photochemical formation of P-bR is not a major source of error in our determination of ΔH_{12}. First, this species is apparently only formed from bR and not K (Gillbro et al., 1977; Kriebel et al., 1979). Accordingly, if P-bR had a significantly different enthalpy than bR, it would produce a significantly different value of ΔH_{12} for the forward (Experiment 1, Table I) than for the reverse (Experiment 2, Table I) reactions. This difference is not observed (within experimental error). Second, P-bR is reported to convert thermally into bR with an activation energy of only $\Delta E = 2.4 \pm 0.2$ kcal mol^{-1} (Kriebel et al., 1979). This observation suggests (but does not prove) that the ground state energy of bR and P-bR are virtually the same, since activation energies are typically much larger than the differences in the reactant and product equilibrium energies when the reactant and product have identical electronic spectra. Accordingly, we conclude that the ground state energies of bR and P-bR are equivalent within the accuracy of our measurements (±2.5 kcal mol^{-1}).

An additional potential source of error is our neglect of fluorescence (Govindjee et al., 1978; Shapiro et al., 1978). In one respect, our neglect of fluorescence is associated with our neglect of a pseudointermediate (P-bR) since it has been argued that all the fluorescence from bR actually occurs from P-bR (Gillbro et al., 1977). This interpretation, however, is not uniformly accepted (Govindjee et al., 1978; Shapiro et al., 1978). Nonetheless, the fact that the fluorescence quantum yield is extremely low ($\sim 2.4 \times 10^{-5}$) (Govindjee et al., 1978) indicates that our neglect of fluoresence is justified.

Systematic Error Due to Uncertainties in the Quantum Yields ϕ_1^f and ϕ_2^r. The quantum yields of the photochemical reactions associated with bR and K have been experimentally determined in a number of investigations (Goldschmidt et al., 1976; Hurley et al., 1977; and Hurley and Ebrey, 1978). The detailed study by Hurley and Ebrey (1978) gave $\phi_1^f = 0.33 \pm 0.05$ and $\phi_2^r = 0.67 \pm 0.04$ for the bR → K and K → bR reactions, respectively, at 77 K. The above values were shown to be wavelength independent and, more interestingly, appear to add up to exactly 1. This latter observation has important mechanistic implications as discussed by Hurley et al. (1977). However, a recent investigation by Suzuki and Callender (1981) indicates that the quantum yields associated with rhodopsin and bathorhodopsin photointerconversion do not add up to exactly 1. Given the fact that earlier investigations of rhodopsin photochemistry had observed a unity summation of the quantum yields for rhodopsin ⇌ bathorhodopsin interconversion, the possibility that a similar deviation from unity for bR ⇌ K photochemistry cannot be dismissed. This question is of paramount importance to the present investigation because small deviations (±0.1) from unit summation will cause large errors (±2 kcal ml^{-1}) in the calculated value of ΔH_{12}. Fortunately, our experimental data provide an opportunity to determine $\phi_1^f + \phi_2^r$ explicitly, as shown in the next section.

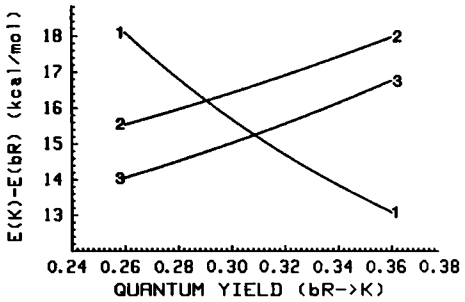

FIGURE 7 The effect of changes in the assumed value of the forward quantum yield, ϕ_1^f, on the calculated values of ΔH_{12} ($E_K - E_{bR}$) for experiments 1, 2, and 3. The curves are calculated assuming $\phi_1^f + \phi_2^r = 1$ and demonstrate the self-compensating nature of the calculated value of ΔH_{12} as a function of uncertainty in the quantum yields ϕ_1^f and ϕ_2^r, provided $\phi_1^f + \phi_2^r = 1$ (see text).

The effect of changes in ϕ_1^f on the measured value of ΔH_{12} is shown in Fig. 7, assuming $\phi_1^f + \phi_2^r = 1$. The salient observation is that our measurement of ΔH_{12} ($E_K - E_{bR}$) as a function of forward, reverse, and mixed reactions is partially self compensating. Whereas the value of ΔH_{12} calculated from the forward reaction (curve 1) decreases with increasing ϕ_1^f, ΔH_{12} is calculated to increase with increasing ϕ_1^f for the reverse (curve 2) and mixed (curve 3) reactions.

Global Optimization of ΔH_{12} and ϕ_2

The three experiments described above provide three determinations of ΔH_{12} as a function of ϕ_1^f and ϕ_2^r. These three experiments can alternatively be used to globally optimize any two of the three variables ΔH_{12}, ϕ_1^f, and ϕ_2^r as a function of the remaining variable. Although the errors inherent in our measurements of Γ^{λ}_{obsvd} will prevent a precise simultaneous determination of two dependent variables, this optimization is worth pursuing.

The three equations used in the optimization are given below

$$\Delta\Gamma_1 = 0.907 - 1 + (\phi_1^f \Delta H_{12}/50.6) \quad (11)$$

$$\Delta\Gamma_2 = 1.281 - 1 - (\phi_2^r \Delta H_{12}/40.9) \quad (12)$$

$$\Delta\Gamma_3 = 1.196 - 0.12 + (0.12\,\phi_1^f \Delta H_{12}/44.5) - 0.88 - 0.88\,\phi_2^r \Delta H_{12}/44.5, \quad (13)$$

where numerical values in italics carry units of kcal mol^{-1}. The salient parameters were optimized to minimize the dimensionless error function

$$\Delta\Gamma^2_{ave} = \tfrac{1}{3}(\Delta\Gamma_1^2 + \Delta\Gamma_2^2 + \Delta\Gamma_3^2) \quad (14)$$

subject to the following constraint

$$0.24 \le \phi_1^f \le 0.40. \quad (15)$$

Although we have three equations (Eqs. 11–13) in three unknowns (ΔH_{12}, ϕ_1^f, and ϕ_2^r), the regression correlation matrix indicates that ϕ_1^f and ϕ_2^r are too strongly correlated to permit definitive assignments of all three variables. The limitation is due to the fact that Eq. 13 is not truly independent of Eqs. 11 and 12 in that it represents a mixture of the forward (Eq. 11) and reverse (Eq. 12) reactions. Accordingly, we are effectively left with only two (independent) measurements. We arbitrarily chose ϕ_1^f as our independent variable and optimized ϕ_2^r and ΔH_{12} for given values of ϕ_1^f. The results are shown in Table III. We further note that our global optimization does not permit a preferred assignment for ϕ_1^f in that a similar minimum value for $\Delta\Gamma^2_{avd}$ is obtained for all values of ϕ_1^f within the range specified by Eq. 15.

TABLE III
GLOBAL OPTIMIZATION OF ϕ_2^r AND ΔH_{12} AS A FUNCTION OF ϕ_1^f*

ϕ_1^f‡	ϕ_2^r§	$\phi_1^f + \phi_2^r$	ΔH_{12}
			kcal mol^{-1}
0.24	0.558 ± 0.086‖	0.798 ± 0.086‖	19.93 ± 3.02‖
0.26	0.605 ± 0.093	0.865 ± 0.093	18.40 ± 2.79
0.28	0.651 ± 0.100	0.931 ± 0.100	17.08 ± 2.59
0.30	0.697 ± 0.107	0.997 ± 0.107	15.94 ± 2.42
0.32	0.744 ± 0.114	1.064 ± 0.114	14.95 ± 2.27
0.33	0.767 ± 0.119	1.097 ± 0.119	14.50 ± 2.21
0.34	0.791 ± 0.122	1.131 ± 0.122	14.07 ± 2.13
0.36	0.837 ± 0.129	1.197 ± 0.129	13.29 ± 2.01
0.38	0.884 ± 0.136	1.264 ± 0.136	12.59 ± 1.91

*ϕ_2^r and ΔH_{12} ($= E_K - E_{bR}$) were obtained by minimizing $\Delta\Gamma^2_{ave}$ (Eq. 14) for values of ϕ_1^f listed in first column.
‡ϕ_1^f is the quantum yield for the bR → K reaction.
§ϕ_2^r is the quantum yield for the K → bR reaction.
‖Error ranges are assigned as ±1 standard deviation based on the regression analysis.

DISCUSSION

Molecular Origins of Energy Storage

The preceding analysis indicates that the primary event of the bR_{568} photocycle stores ~16 kcal mol^{-1} of energy in the K intermediate. This value is significantly smaller than the ~35 kcal mol^{-1} stored in the primary event of the (bovine) rhodopsin photobleaching sequence (Cooper, 1979). There is compelling evidence that the primary photochemical events associated with both rhodopsin and bacteriorhodopsin involve isomerization of the retinyl chromophore (Honig, 1982; Birge, 1981; Tsuda et al., 1980; Ottolenghi, 1980). Although deuterium isotope effects suggest that a proton translocation is also associated with these primary processes, it is likely that the translocation occurs as a ground state process following isomerization (Honig, 1982). Although the chronology of these events is still a subject of debate, we can be reasonably confident that a major portion of the energy uptake in the primary event is associated with isomerization (Birge, 1981). What remains to be explained is the molecular origins of the energy storage.

Honig and co-workers have long suggested that the separation of the protonated Schiff base from its counterion as a consequence of photoisomerization could account for much of the energy uptake associated with the primary event (Honig, 1982; Honig, et al., 1979; Rosenfeld et al., 1977). A theoretical investigation of energy storage in the primary event of rhodopsin by Birge and Hubbard (1980, 1981) predicted that bathorhodopsin has a ground state energy ~26 kcal mol^{-1} larger than rhodopsin. The energy storage was partitioned into two components, compression of the lysine residue (~14 kcal mol^{-1}) and charge separation (~12 kcal mol^{-1}). Warshel and Barboy (1982), however, have proposed an empirical protein constraint model of energy storage which predicts that a much more significant fraction of the energy storage in bathorhodopsin is associated with deformation of the protein cavity. These authors suggest that the strain energy can be approximated by the formula

$$V_{strain} = \tfrac{1}{2} K_p \sum_i^N (\Delta r_i)^2, \qquad (16)$$

where K_p is an empirical force constant of the protein, Δr_i is the displacement of atom i due to isomerization of the chromophore, and the summation extends over all N atoms of the chromophore. Warshel and Barboy suggest values of K_p in the range 0.25–0.5 kcal mol^{-1} $Å^{-2}$ and calculate $\Sigma_i \Delta r_i^2 = 169$ $Å^2$ to yield strain energies of 21–42 kcal mol^{-1}. They suggest that $K_p \sim 0.25$ is "a very conservative estimate" and therefore a significant fraction of energy storage in bathorhodopsin is associated with deformation of the protein cavity.

The primary event of the bacteriorhodopsin photocycle involves isomerization of the all-*trans* chromophore to the 13-*cis* configuration (Tsuda et al., 1980). The maximum value of $\Sigma \Delta r_i^2$ for this isomerization is only 60 $Å^2$. This value assumes a full 180° to 0° rotation of the 13,14 double bond without any conformational minimization, which will invariably occur to decrease the strain energy and decrease $\Sigma \Delta r_i^2$. Accordingly, if we assume the same protein constraint parameters used by Warshel and Barboy in simulating the rhodopsin → bathorhodopsin process, we calculate a strain energy of 7.5 kcal mol^{-1} ($K_p = 0.25$) to 15 kcal mol^{-1} ($K_p = 0.5$). The observation that a value of $K_p = 0.5$ kcal mol^{-1} yields a bathorhodopsin strain energy that is larger than the total relative energy, but yields a K strain energy that is less than the relative energy of K, indicates one of two things: either the protein constraint force constant is significantly larger for bacteriorhodopsin than rhodopsin, or charge separation is a significant source of the energy storage in K. Although we cannot categorically exclude the former, we suggest that the latter explanation is the more plausible. We note that the charge separation energy is a linear function of distance (Δr_i), whereas the strain energy (based on Eq. 16) is a function of the square of the atomic distances (Δr_i^2). Accordingly, if charge separation were the major source of energy storage in both bathorhodopsin and K, we would expect bathorhodopsin to have roughly twice the energy as K relative to their respective precursors. If protein deformation were the major source of energy storage, we would expect bathorhodopsin to have at least 2.8 and perhaps 4 times the relative energy as K with reference to their respective precursors. The former ratio is closer to that observed and we conclude that at least one-half of the energy storage in K is associated with charge separation.

Energy Storage and the Subsequent Dark Reactions

The photocalorimetry of bacteriorhodopsin at room temperature has been studied by a number of investigators (LeGrange et al., 1982; Garty et al., 1982; Ort and Parson, 1979). The detailed study by Ort and Parson (1979) is particularly interesting because it indicates that metastable species with relative enthalpies of 15–20 kcal mol^{-1} are present 100 μs after excitation. Following the chronology shown in Fig. 1, we conclude that a significant fraction of the bR_{568} molecules excited have already reached L_{550} after 100 μs. (Under the experimental conditions used by Ort and Parson, it is unlikely that the enthalpy associated with the instantaneous (100 μs) volume change is associated with M_{412}.) The enthalpies of L_{550} and K therefore appear to be nearly identical. Two resolutions to this apparent anomaly are possible: (*a*) the dark reaction $K_{610} \rightarrow L_{550}$ is entropy driven or (*b*) the relative energy of K_{610} measured at 77 K (~16 kcal mol^{-1}) reflects a slow (~10 s) protein relaxation that is not fully accomplished at room temperature before formation of the L_{550} intermediates. These two possibilities may, of course, both contribute, but a full resolution of this question must await further study.

CONCLUSIONS

(*a*) The primary step in the photocycle of light-adapted bacteriorhodopsin stores 15.8 ± 2.5 kcal mol^{-1} in the K intermediate at 77 K. This enthalpy corresponds to ~30% of the abosrbed photon energy at the 568-nm absorption maximum. (*b*) The quantum yields for photochemical interconversion of bR → K (ϕ_1^f) and K → bR (ϕ_2^r) sum to unity within experimental error ($\phi_1^f + \phi_2^r = 1.02 \pm 0.19$) for values of ϕ_1^f in the range 0.28–0.33. (*c*) A significant fraction (>0.5) of the energy storage in the primary event is associated with charge separation accompanying isomerization of the retinyl protonated Schiff base chromophore.

We gratefully acknowledge generous gifts of *Halobacterium halobium* from Professors Walther Stoeckenius and Richard Mathies, and thank Dr. Alan Cooper and Professors Barry Honig, William Parson, Hartland Schmidt, and Walther Stoeckenius for helpful discussions. We also thank Mr. Gene Ethridge for technical assistance and advice during the construction of the calorimeter.

T. M. Cooper acknowledges an Earle C. Anthony graduate student fellowship. This work was supported in part by grants from the National

Institutes of Health (EY-02202) and the National Science Foundation (CHE-7916336).

Received for publication 14 September 1982 and in final form 13 December 1982.

REFERENCES

Becher, B., and J. Y. Cassim. 1975. Improved isolation procedures for the purple membrane of *H. Halobium*. *Prep. Biochem.* 5:161–178.

Bennett, J. A., and R. R. Birge. 1981. Two-photon spectroscopy of diphenylbutadiene. The nature of the lowest-lying $^1A_g^{*-}$ $\pi\pi^*$ state. *J. Chem. Phys.* 73:4234–4246.

Birge, R. R. 1981. Photophysics of light transduction in rhodopsin and bacteriorhodopsin. *Annu. Rev. Biophys. Bioeng.* 19:315–54.

Birge, R. R. 1983. One-photon and two-photon excitation spectroscopy. *In* Ultrasensitive Laser Spectroscopy. D. S. Kliger, editor. Academic Press, Inc., New York. 109–174.

Birge, R. R., and L. M. Hubbard. 1980. Molecular dynamics of *cis-trans* isomerization in rhodopsin. *J. Am. Chem. Soc.* 102:2195–2205.

Birge, R. R., and L. M. Hubbard. 1981. Molecular dynamics of *trans-cis* isomerization in bathorhodopsin. *Biophys. J.* 34:517–534.

Cooper, A. 1979. Energy uptake in the first step of visual excitation. *Nature (Lond.)*. 282:531–533.

Cooper, A. 1982. Calorimetric measurements of light-induced processes. *Meth. Enzymol.* 88:667–673.

Garty, H., S. R. Caplan, and D. Cahen. 1982. Photoacoustic photocalorimetry and spectroscopy of *Halobacterium Halobium* purple membranes. *Biophys. J.* 37:405-415.

Gillbro, T., and V. Sundström. 1983. Picosecond kinetics and a model for the primary events of bacteriorhodopsin. *Photochem. Photobiol.* In press.

Gillbro, T., A. N. Kriebel, and U. P. Wild. 1977. The origin of the red emission of light adapted purple membrane of *H. Halobium*. *FEBS (Fed. Eur. Biochem. Soc.) Lett.* 78:57–60.

Goldschmidt, C. R., M. Ottolenghi, and R. Korenstein. 1976. On the primary quantum yield in the bacteriorhodopsin photocycle. *Biophys. J.* 16:839–843.

Govindjee, R., B. Becher, and T. Ebrey. 1978. The fluorescence from the chromophore of the purple membrane protein. *Biophys. J.* 22:67–77.

Honig, B. 1982. Theoretical aspects of photoisomerization in visual pigments and bacteriorhodopsin. *In* Biological Events Probed by Ultrafast Laser Spectroscopy. R. R. Alfano, editor. Academic Press, Inc., New York 281–296.

Honig, B., V. Dinur, K. Nakanishi, V. Balogh-Nair, M. A. Gawinowicz, M. Arnaboldi, and M. G. Motto. 1979. An external point-charge model for wavelength regulation in visual pigments. *J. Am. Chem. Soc.* 101:7084–7086.

Hurley, J. B., and T. G. Ebrey. 1978. Energy transfer in the purple membrane of *Halobacterium Halobium*. *Biophys. J.* 22:49–66.

Hurley, J. B., T. G. Ebrey, B. Honig, and M. Ottolenghi. 1977. Temperature and wavelength effects on the photochemistry of rhodopsin, isorhodopsin, bacteriorhodopsin, and their photoproducts. *Nature (Lond.)*. 270:540–542.

Kaufmann, K. J., V. Sunström, T. Yamane, and P. M. Rentzepis. 1978. Kinetics of the 580-nm ultrafast bacteriorhodopsin transient. *Biophys. J.* 22:121–124.

Kriebel, A. N., T. Gillbro, and U. P. Wild. 1979. A low temperature investigation of the intermediates of the photocycle of light-adapted bacteriorhodopsin. Optical absorption and fluorescence measurements. *Biochim. Biophys. Acta.* 546:106–120.

LeGrange, J., D. Cahen, and S. R. Caplan. 1982. Photoacoustic calorimetry of purple membrane. *Biophys. J.* 37:4–6.

Lozier, R., and W. Niederberger. 1977. The photochemcial cycle of bacteriorhodopsin. *Fed. Proc.* 36:1805–1809.

Lozier, R. H., R. A. Bogomolni, and W. Stoeckenius. 1975. Bacteriorhodopsin: a light-driven proton pump of *Halobacterium Halobium*. *Biophys. J.* 15:955–962.

Ort, D. R., and W. W. Parson. 1979. Enthalpy changes during the photochemical cycle of bacteriorhodopsin. *Biophys. J.* 25:355–364.

Ottolenghi, M. 1980. The photochemistry of rhodopsins. *In* Advances in Photochemistry. J. N. Pitts, Jr., G. S. Hammond, K. Gollnick, and D. Grosjean, editors. John Wiley and Sons, Inc., New York. 97–200.

Rosenfeld, T., B. Honig, M. Ottolenghi, J. B. Hurley, and T. G. Ebrey. 1977. On the role of the protein in the photoisomerization of the visual pigment chromophore. *Pure Appl. Chem.* 49:341–351.

Shapiro, S. L., A. J. Campillo, A. Lewis, G. J. Perreault, J. P. Spoonhower, R. K. Clayton, and W. Stoeckenius. 1978. Picosecond and steady state, variable intensity and variable temperature emission spectroscopy of bacteriorhodopsin. *Biophys. J.* 23:383–393.

Stoeckenius, W., R. H. Lozier, and R. A. Bogomolni. 1979. Bacteriorhodopsin and the purple membrane of *Halobacteria*. *Biochim. Biophys. Acta.* 505:215–278.

Suzuki, T., and R. H. Callender. 1981. Primary photochemistry and photoisomerization of retinal at 77 K in cattle and squid rhodopsin. *Biophys. J.* 34:261–270.

Tsuda, M., M. Glaccum, B. Nelson, and T. G. Ebrey. 1980. Light isomerizes the chromophore of bacteriorhodopsin. *Nature (Lond.)*. 287:351–353.

Warshel, A., and N. Barboy. 1982. Energy storage and reaction pathways in the first step of the vision process. *J. Am. Chem. Soc.* 104:1469–1476.